



# Design, synthesis and biochemical evaluation of novel carbonic anhydrase inhibitors triggered by structural knowledge on hCA VII

Francesca Mancuso<sup>a,\*</sup>, Anna Di Fiore<sup>b</sup>, Laura De Luca<sup>a</sup>, Andrea Angeli<sup>c</sup>,  
Giuseppina De Simone<sup>b</sup>, Claudiu T. Supuran<sup>c</sup>, Rosaria Gitto<sup>a,\*</sup>

<sup>a</sup> Dipartimento CHIBIOFARAM, Università degli Studi di Messina, Viale Palatucci, Polo Didattico SS. Annunziata, 98168 Messina, Italy

<sup>b</sup> Istituto di Biostrutture e Bioimmagini-CNR, Via Mezzocannone 16, 80134 Napoli, Italy

<sup>c</sup> Dipartimento NEUROFARBA, Università di Firenze, Via Ugo Schiff 6, 50019 Sesto Fiorentino, Italy

## ARTICLE INFO

### Keywords:

Carbonic Anhydrase Inhibitors (CAIs)  
X-ray crystallography  
Benzenesulfonamides  
Docking simulations

## ABSTRACT

To tackle the challenge of isoform selectivity, we explored the entrance of the cavity for selected druggable human Carbonic Anhydrases (hCAs). Based on X-ray crystallographic studies on the 4-(4-(2-chlorobenzoyl)piperazine-1-carbonyl)benzenesulfonamide in complex with the brain expressed hCA VII (PDB code: 7NC4), a series of 4-(4(hetero)aroylpiperazine-1-carbonyl)benzene-1-sulfonamides has been developed. To evaluate their capability to fit the hCA VII catalytic cavity, the newer benzenesulfonamides were preliminary investigated by means of docking simulations. Then, this series of thirteen benzenesulfonamides was synthesized and tested against selected druggable hCAs. Among them, the 4-(4-(furan-2-carbonyl)piperazine-1-carbonyl)benzenesulfonamide showed remarkable affinity towards hCA VII ( $K_i$ : 4.3 nM) and good selectivity over the physiologically widespread hCA I when compared to Topiramate (TPM).

## 1. Introduction

Carbonic Anhydrases (CAs, EC 4.2.1.1) are a family of metalloenzymes regulating the cellular concentration of bicarbonate and proton through the reversible hydration of carbon dioxide.<sup>1</sup> Twelve catalytically active isoforms have been so far identified in humans; these isoforms differ for catalytic efficiency and oligomeric structure as well as tissue and cellular distribution.<sup>2</sup> hCAs control both physiological and pathological processes (cancer, epilepsy, obesity, glaucoma);<sup>3</sup> therefore, many of them represent well-recognized targets to develop selective hCA inhibitors (hCAIs) as theranostic agents for above-mentioned diseases.<sup>1,4–11</sup>

The crystal structures of the majority of human isoforms have been determined, both in apo-state and in complex with various chemotypes,<sup>1</sup> highlighting that the active site is localized in a conical cavity with a zinc ion positioned at the bottom and coordinated by three histidine residues (H94, H96, and H119) and a water molecule/hydroxide ion.<sup>12</sup> The middle portion of the cavity is composed of two halves comprising crucial hydrophobic and hydrophilic residues; these two different walls

control the entrance of CO<sub>2</sub> and release of bicarbonate after the hydration reaction. The catalytic process is supported by H64, a residue operating as a proton shuttle and that is generally conserved in all catalytic active hCAs with the exception of hCA III, VA and VB isoforms.<sup>12</sup>

The most studied CAIs belong to the class of sulfonamides and their bioisosters. These compounds are endowed by the capability to inhibit the binding of H<sub>2</sub>O/OH<sup>-</sup> to zinc ion. Furthermore, the sulfonamide zinc binder group (ZBG) also establishes additional polar contacts with T199 residue within the catalytic cavity. In addition to the crucial interactions with metal ion region, effective CAIs create a network of contacts with hydrophobic/hydrophilic residues in the middle area of the cavity. Finally, the classical sulfonamide CAIs possess a so-called “tail” that enables each ligand to interact with the entrance of active site cavity which is lined by amino acidic residues that are not highly conserved.<sup>12</sup> As consequence, the design of isoform/disease specific CAIs generally targets the middle and/or top areas of CA cavity.

The drug development process focused on CAIs led to the identification of several agents currently in therapy or early stage of clinical trials. The first-generation molecules acetazolamide (AAZ, 1) and

*Abbreviations:* AAZ, acetazolamide; CA, carbonic anhydrase; CAIs, carbonic anhydrase inhibitors; HBTU, 2-(1H-Benzotriazole-1-yl)-1,1,3,3-tetramethyluronium hexafluorophosphate, TPM topiramate.

\* Corresponding authors.

E-mail address: [francesca.mancuso@unime.it](mailto:francesca.mancuso@unime.it) (F. Mancuso).

<https://doi.org/10.1016/j.bmc.2021.116279>

Received 5 May 2021; Received in revised form 9 June 2021; Accepted 11 June 2021

Available online 17 June 2021

0968-0896/© 2021 Elsevier Ltd. All rights reserved.

topiramate (TPM, **2**) are well-known CAIs toward druggable isoforms (see Figure 1). For instance, these two therapeutics inhibit brain diffused hCA VII isoform, so that they might be clinically employed for treatment of epilepsy and other neurological disorders.<sup>13–15</sup> More recently, the 4-ureido-benzenesulfonamide derivative SLC-0111 (**3**) entered clinical evaluation as therapeutic agent for hypoxic tumors and its potential is related to highest affinity toward hCA IX/hCA XII isoforms.<sup>9,16–25</sup>

In search of CA isoform selectivity, we have developed a library of substituted piperazine-1-carbonyl-benzenesulfonamides which inhibited selected isoforms (e.g. hCA VII, hCA IX, hCA XII and hCA XIV).<sup>13,14,26,27</sup> For several 4-(4-arylpiperazine-1-carbonyl)benzene-1-sulfonamides (e.g. compound **4**) and related 4-(4-arylpiperazine-1-carbonyl)benzene-1-sulfonamides (e.g. compound **5**) the crystal structure in complex with the target enzyme evidenced the ligands bound within the hCA II cavity.<sup>28,29</sup> As expected, the sulfonamide functionality acted as ZBG, whereas, the piperazine core established favorable contacts with residues paving the two walls of the middle region of the cavity. Finally, the remaining aromatic fragment played the role of the so-called “tail” interacting with rim of the cavity.

Inhibition assays have demonstrated that the prototype compound **5** was a highly effective inhibitor against hCA II, hCA VII, hCA IX and hCA XII revealing that the introduction of a suitable substituent on the aromatic “tail” was able to improve the affinity for hCA VII or hCA IX/XII.<sup>28</sup> These findings prompted us to continue to explore the class of 4-(4-arylpiperazine-1-carbonyl)benzene-1-sulfonamides with the aim to identify newer selective hCAIs for target-therapy for cancer or neurological diseases. Our idea was to acquire further structural information about the optimal pattern of structural modifications to ameliorate CA affinity/selectivity toward druggable hCAs.

## 2. Results and discussion

Herein, in the first step of our study we solved the crystal structure of the complex that hCA VII forms with the previously reported active compound 4-(4-(2-chlorobenzoyl)piperazine-1-carbonyl)benzenesulfonamide (**6**, PDB code 7NC4).<sup>28</sup> Crystals were obtained by the soaking technique and the structure was determined at 1.60 Å and refined to final crystallographic R-work and R-free values of 0.196 and 0.214, respectively (for data collection and refinement statistics see Table S1 in Supplementary Material).

Electron density maps ( $|Fo-Fc|$  and  $|2Fo-Fc|$  maps) were calculated at various stages of the crystallographic refinement revealing features compatible with the presence of compound **6** within hCA VII active site (Figure 2). These maps were very well defined for the carbonyl-benzenesulfonamide portion, while a higher disorder was observed for 2-chlorobenzoylpiperazine moiety, thus suggesting a certain degree of

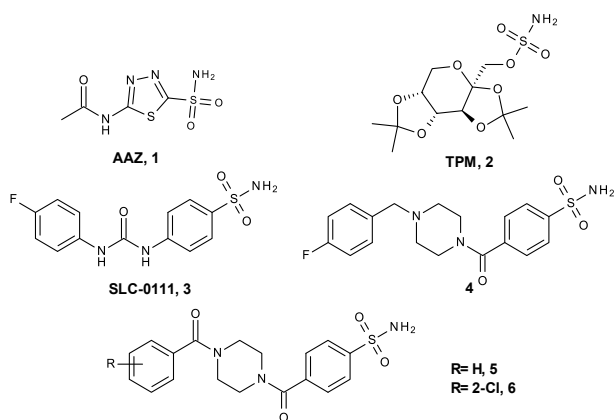


**Figure 1.** Chemical structures of some hCAIs: AAZ (**1**), TPM (**2**), SLC-0111 (**3**), 4-(4-(4-fluorobenzoyl)piperazine-1-carbonyl)benzenesulfonamide (**4**), and 4-(4-arylpiperazine-1-carbonyl)benzenesulfonamide derivatives (**5–6**).

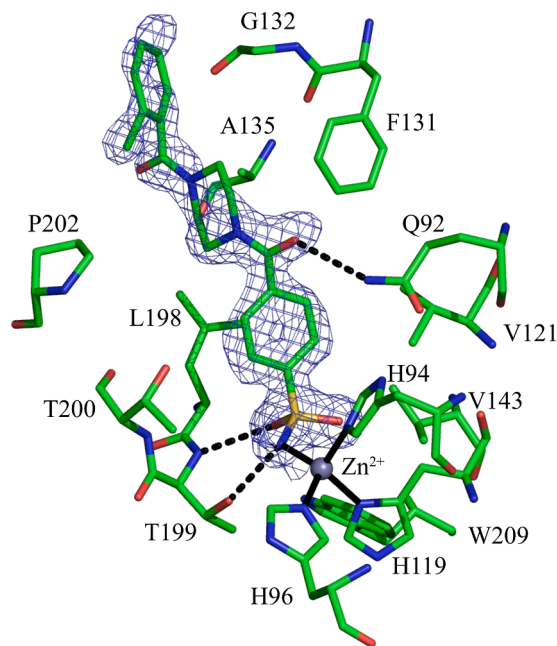


**Figure 2.** Sigma-A weighted  $|2Fo-Fc|$  simulated annealing omit map (contoured at 1.0  $\sigma$ ) of inhibitor **6** bound to hCA VII active site (PDB code 7NC4). The catalytic zinc ion is represented as a gray sphere. The zinc ion coordination (black continuous lines), hydrogen bonds (black dashed lines) and residues involved in van der Waals interactions are also depicted. The figure was generated by using PyMOL program.

inhibitor flexibility within the enzyme active site. As already observed for other hCAIs containing the sulfonamide moiety,<sup>28</sup> compound **6** coordinated the catalytic zinc ion through the deprotonated nitrogen atom of the primary sulfonamide group, displacing the zinc-bound water molecule/hydroxide ion and forming further hydrogen bond interactions with T199 residue (Figure 2). The benzenesulfonamide core established strong van der Waals interactions with the following amino acids Q92, H94, V121, V143, L198, T199, T200 and W209, whereas the carbonyl group was engaged into a hydrogen bond with NE2 atom of Q92 side chain. Finally, the 2-chlorobenzoylpiperazine tail was oriented toward the rim of the catalytic cavity establishing several van der Waals interactions with F131, G132 and A135, L198 and P202 residues as shown in Figure 2.

Starting from this structural information, we decided to investigate the effect of the substitution of the 2-chlorobenzoyl fragment with several (hetero)aryl fragments containing naphthalene, thiophene, furan and pyrrole rings (see compounds **7a–m** in Figure 3). The choice was addressed to exploit a set of heteroaryl fragments possessing a different degree of lipophilicity, H-bond donor/acceptor ability, polar surface area (polarity) as well as other key features to optimize ADME/Tox properties.

The binding poses of these molecules into hCA VII active site was then explored by means of a docking approach using the crystallographic coordinates of the hCA VII/**6** adduct as reference structure. The docking protocol (see Supplementary Material) was first validated through self-docking of derivative **6**, whose best docking pose was in good agreement with the experimental structure.

The visual inspection of the predicted binding poses of compounds **7a–m** confirmed their ability to nicely fit the catalytic cavity of hCA VII, (Figure 4). For all docked compounds the arylsulfonamide moiety was located in the bottom of the cavity and participated in the interaction with zinc ion, as shown in the structure of the hCA VII/**6** adduct reported in Figure 2. The piperazine core occupied the middle region of the cavity; whereas a slight variation of the tail orientation was observed for several compounds, which projected the heteroaromatic substituent

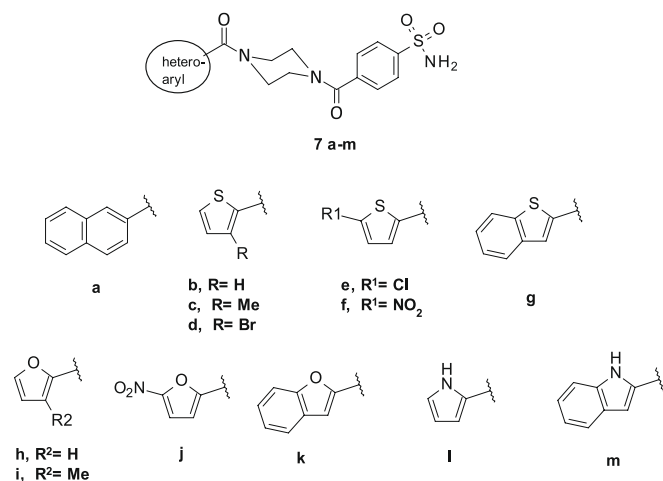


**Figure 3.** Designed 4-(4-(hetero)aryl)piperazine-1-carbonyl)benzene-1-sulfonamides **7a-m**.

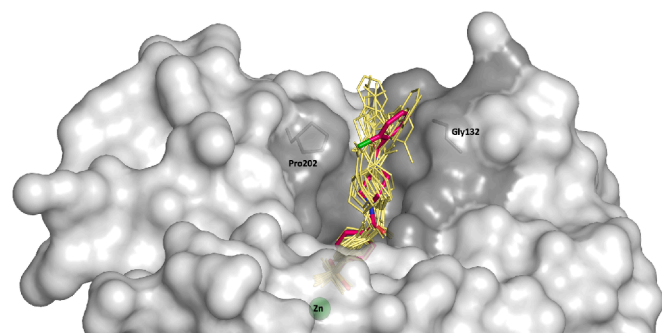
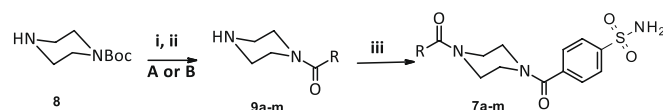


**Figure 4.** Superposition of the binding pose of benzenesulfonamides **7a-m** (pale yellow stick) with 4-(4-(2-chlorobenzoyl)piperazine-1-carbonyl)benzenesulfonamide (**6**) (hot pink stick) bound to hCA VII active site. The protein is depicted as light grey surface. Residues around 4 Å by compound **6** are colored in dark grey. Zinc ion is reported as green sphere. The figure was generated by using PyMOL program. (For interpretation of the references to colour in this figure legend, the reader is referred to the web version of this article.)

toward P202 residue rather than toward G132. Considering that the different orientation of the tail could confer a different inhibition and selectivity profile to the new 4-(4-(hetero)aryl)piperazine-1-carbonyl)benzene-1-sulfonamides with respect to the prototype **6**, we decided to synthesize derivatives **7a-m** following an optimized synthetic procedure.<sup>28</sup>

As shown in **Scheme 1** the heteroaryl(piperazin-1-yl)methanones **9a-m** intermediates were obtained by the coupling reaction between the commercially available 1-Boc-piperazine (**8**) and the suitable heteroaryl chloride or carboxylic acid derivatives, followed by Boc group removal in a *one pot* route. Then, **9a-m** reacted with activated 4-sulfamoylbenzoic acid providing the title 4-(4-(hetero)aryl)piperazine-1-carbonyl)benzene-1-sulfonamides **7a-m** in good yields. The described synthetic protocol was optimized by using microwaves irradiation thus



**Scheme 1.** Reagents and conditions: (i) pathway A RCOCl, DIPEA, DCM/DMF (2:1, v/v), MW, 10 min or pathway B RCO<sub>2</sub>H activated by HBTU in DCM/DMF (2:1, v/v), MW, 1 min, then DIPEA, MW, 25 min; and (ii) TFA dropwise, 0 °C to rt, MW, 5 min; (iii) activated 4-sulfamoylbenzoic acid by HBTU in DMF, MW, 1 h, then TEA, rt, overnight (overall yield 32–73%).

reducing the reaction time from more than twelve hours to twenty-five minutes. All the final compounds were fully characterized by spectroscopic (<sup>1</sup>H-NMR and <sup>13</sup>C NMR) and elemental analyses (see **Supporting Material**).

The newly synthesized compounds were analyzed by using a stopped-flow CO<sub>2</sub> hydrase assay for their inhibitory potency against the widespread hCA I and hCAII, and the selected isoforms hCA VII, hCA IX and hCA XII. Inhibition data are listed in **Table 1** in comparison with **1** and **2** and the prototypes **5** and **6**.

A careful SAR analysis of data reported in **Table 1** suggests:

- The 4-(4-(hetero)aryl)piperazine-1-carbonyl)benzenesulfonamides **7a-m** proved to be inhibitors of hCA I showing  $K_i$  values ranging from 3.4 to 454.8 nM. In detail, compounds **7b** (2-thienyl substituted) and **7h** (2-furyl substituted) acted as weak inhibitors of the dominant hCA I compared to the parent compounds **5** and **6**, suggesting that the introduction of these two five-membered heteroaromatic rings was detrimental for the hCA I affinity. However, the introduction of a further substituent on the thiophene ring as in compounds **7c-7e** significantly improved the inhibition properties against this isoform.
- All the investigated compounds strongly affected activity of the cytosolic hCA II ( $K_i$  values from 1.2 to 38 nM). In particular, the introduction of several substituents as well benzene fused ring on 2-thiophene (**7b**), 2-furan (**7h**) or 2-pyrrole (**7l**) rings led to an improvement of affinity against this isoform. Among them, compounds **7d** (R = 3-bromothiophen-2-yl) and **7e** (R = 5-chlorothiophen-2-yl) resulted the most active hCA II inhibitors ( $K_i$  values of 1.8 and 1.2 nM, respectively).
- Notably, all newly synthesized compounds **7a-m** demonstrated high inhibitory effects against the target brain related hCA VII with  $K_i$  values spanning from 4.3 to 84 nM. Specifically, the best outcome has been obtained for the furan-tailed compound **7h**, which although less active than the prototype **6** ( $K_i$  values of 4.3 vs 2.9 nM) showed a better selectivity ratio over hCA I and hCA II comparable with those of the anticonvulsant **2**.
- The *trans*-membrane isoform hCA IX was poorly inhibited by compounds **7a-l**, suggesting that the introduction of different aromatic system in place of benzene ring (*cfr.* compound **5**) is highly detrimental for the interaction with this isoform. Although the hCA IX inhibition profile resulted the most affected for the inclusion of different tails, a flat structural correlation was

**Table 1**

Inhibition data of human CA I, II, VII, IX and XII with compounds **5**, **6**, **7a-m** and the known inhibitors AAZ and TPM.

	$K_i$ nM <sup>a</sup>				
	hCA I	hCA II	hCA VII	hCA IX	hCA XII
<b>5</b>	69.1 ± 6.9	3.7 ± 0.4	70.7 ± 7.1	37.1 ± 3.7	8.5 ± 0.8
<b>6</b>	94.4 ± 9.2	5.6 ± 0.6	2.9 ± 0.3	62.2 ± 6.2	63.1 ± 6.3
<b>7a</b>	66.2 ± 6.3	3.4 ± 0.3	8.3 ± 0.8	2989 ± 295	91.8 ± 9.2
<b>7b</b>	425.8 ± 4.0	38.0 ± 3.5	21.5 ± 2.1	3279 ± 324	644.3 ± 64.4
<b>7c</b>	8.1 ± 0.8	14.2 ± 1.3	7.1 ± 0.7	2920 ± 290	481.9 ± 48.2
<b>7d</b>	6.4 ± 0.6	1.8 ± 0.2	56.4 ± 5.6	124.7 ± 12.5	6.2 ± 0.6
<b>7e</b>	3.4 ± 0.3	1.2 ± 0.1	84.0 ± 8.2	381.5 ± 37.1	7.1 ± 0.7
<b>7f</b>	12.7 ± 1.1	4.4 ± 0.4	57.9 ± 5.1	171.2 ± 17.1	9.0 ± 0.9
<b>7g</b>	34.8 ± 3.2	4.1 ± 0.4	68.3 ± 6.2	97.9 ± 9.9	9.1 ± 0.9
<b>7h</b>	454.8 ± 45.5	33.7 ± 3.4	4.3 ± 0.4	3175 ± 312	494.6 ± 49.5
<b>7i</b>	78.3 ± 7.6	20.2 ± 2.0	15.5 ± 1.5	3045 ± 301	49.6 ± 5.0
<b>7j</b>	14.8 ± 1.3	4.0 ± 0.4	9.4 ± 0.9	976.2 ± 97.6	30.7 ± 3.1
<b>7k</b>	51.9 ± 5.1	2.8 ± 0.3	7.2 ± 0.7	2938 ± 293	240.6 ± 24.1
<b>7l</b>	47.7 ± 4.4	6.8 ± 0.7	7.6 ± 0.8	276.9 ± 27.7	16.7 ± 1.7
<b>7m</b>	73.2 ± 7.3	5.8 ± 0.6	82.5 ± 8.2	9.2 ± 0.9	66.9 ± 6.7
<b>1</b>	250 ± 25.0	12.5 ± 1.2	2.5 ± 0.2	25.8 ± 2.6	5.7 ± 0.6
<b>2</b>	250 ± 25.0	10 ± 1.0	0.9 ± 0.09	58 ± 5.8	ND

<sup>a</sup> Errors in the range of ± 10% (SD) of the reported value, from 3 different assays. Recombinant hCA I, hCA II and hCA VII full-length and hCA IX, hCA XII catalytic domains were used.

observed. Unique in this series, the 2-indolyl derivative **7m** unexpectedly inhibited hCA IX demonstrating very low nanomolar activity ( $K_i$  value of 9.2 nM).

- v. The nature of (hetero)aromatic moiety demonstrated a relevant role in inhibition of hCA XII isoform. In some case the introduction of appropriate substituents on thienyl ring led to a significant enhancement of activity up to low nanomolar concentrations thus restoring the same potency of prototype **5** as observed for compounds **7d**, **7e**, **7f** and **7g**.

Taken together these results suggest that even small modifications of (hetero)aroyl tail may induce a significant effect on the inhibition potency as well as on the isoform selectivity against the different CA isoforms. Based on the comparison of calculated physicochemical properties (<http://www.swissadme.ch>) and the results of structure-affinity relationship analysis, it was observed that the hCA affinity/selectivity of sulfonamides **9a-m** did not associated with their different lipophilic properties as well as with the presence of heterocycles containing multiple H-bond acceptor/donor functionalities. In terms of calculated PK properties, except for polar nitro-substituted compounds (**7f** and **7j**), we generally found that the studied compounds were predicted orally bioavailable (see [Supporting Material](#)). However, they possessed poor estimated adsorption to CNS, therefore the exploitation of active hCA VII inhibitor **7h** might result impaired.

### 3. Conclusions

The current study reports a structure-inspired drug design which led to the identification of a class of 4-(4-(hetero)aroylpiperazine-1-carbonyl)benzene-1-sulfonamides as human CAIs. This library of thirteen compounds has been designed by the replacement of benzene ring of the known hCA inhibitors 4-(4-aroylpiperazine-1-carbonyl)benzene-1-sulfonamide with a variable hetero-aromatic system. In general, these compounds induced a consistent inhibition of the selected hCAs and  $K_i$  spanned from a low micromolar to a low nanomolar range. Specifically, the 4-(4-(furan-2-carbonyl)piperazine-1-carbonyl)benzenesulfonamide (**7h**) turned out as the most potent hCA VII inhibitor of the study and proved to be selective for hCA VII over other studied isoforms.

## 4. Experimental section

### 4.1. X-ray crystallography

Crystals of the hCA VII/6 adduct were obtained by using the soaking technique. A mutated form of hCA VII isoform, where the cysteine residues in position 183 and 217 were mutated to serines, was used, since this mutant is more easily crystallized.<sup>30</sup> In particular, crystals of unbound protein were grown at room temperature by the hanging drop vapor diffusion technique using a protein concentration of 5 mg/mL (in 20 mM Tris-HCl pH 8.0 and 100 mM NaCl) and 18% v/v Peg3350, 0.2 M sodium acetate and 0.1 M Tris pH 8.5 as precipitant solution. A few hCA VII crystals were then transferred in a 2  $\mu$ L drop of freshly prepared precipitant solution containing also the inhibitor at the concentration of 40 mM and glycerol (25% v/v) as cryoprotectant. These crystals were kept in the soaking solution for one hour and then flash-frozen in liquid nitrogen.

X-ray diffraction data were collected by using a copper rotating anode generator developed by Rigaku, equipped with a Rigaku Saturn CCD detector. Diffraction data were indexed, integrated and scaled using the HKL2000 software package.<sup>31</sup> Data collection statistics are reported in [Table 1S](#).

The initial phases of the structure were calculated using the atomic coordinates of the unbound hCA VII (PDB accession code 6G4T) with waters removed.<sup>32</sup>

The structure was refined using the program CNS4,<sup>33,34</sup> whereas model building, and map inspections were performed using the program

O.<sup>35</sup> The topologies and parameters for the inhibitor molecule were generated using the PRODRG server.<sup>36</sup> Several rounds of energy minimization and B-factor refinement alternated with manual rebuilding were necessary to reduce the crystallographic R-work/R-free values to 0.196/0.214. Refinement statistics are summarized in [Table 1S \(Supplementary Material\)](#).

The stereochemical quality of the model was finally checked using Procheck and Whatcheck programs.<sup>37</sup> Coordinates and structure factors have been deposited in the Protein Data Bank (accession code 7NC4).

### 4.2. Docking studies

Docking studies were performed by Gold software V 2020.2.0<sup>35</sup> using as starting structure the crystal structure of hCA VII in complex with the inhibitor **6** (PDB code 7NC4) reported in the previous section. Ligand and water molecules were discarded and hydrogen atoms were added to protein with Discovery Studio Visualiser V20. Ligand structures were built by VegaZZ software<sup>38</sup> and energy minimized by employing a conjugate gradient minimization by AMMP calculation. The region of interest used by Gold program was defined in order to contain residues within 10 Å from the original position of the ligand in the X-ray structure. A scaffold constraint (penalty = 5.0) was used to restrict the solutions in which the sulfonamide moiety was able to coordinate the metal within the catalytic binding site. ChemPLP was chosen as fitness function and the standard default settings were used in all calculations. Ligands were submitted to 100 genetic algorithm runs and the "allow early termination" command was deactivated. Results differing by less than 0.75 Å in ligand-all atom RMSD, were clustered together. The best GOLD-calculated conformation was considered both for analysis and representation.

### 4.3. Chemistry

All reagents were used without further purification and bought from common commercial suppliers. Microwave-assisted reactions were carried out in a Focused Microwave TM Synthesis System, Model Discover (CEM Technology Ltd Buckingham, UK). Melting points were determined on a Buchi B-545 apparatus (BUCHI Labortechnik AG Flawil, Switzerland) and are uncorrected. By combustion analysis (C, H, N) carried out on a Carlo Erba Model 1106-Elemental Analyzer we determined the purity of synthesized compounds; the results confirmed a  $\geq$  95% purity. Merck Silica Gel 60 F254 plates were used for analytical TLC (Merck KGaA, Darmstadt, Germany.). <sup>1</sup>H-NMR and <sup>13</sup>C-NMR spectra were measured in dimethylsulfoxide-*d*<sub>6</sub> (DMSO-*d*<sub>6</sub>) with a Varian Gemini 500 spectrometer (Varian Inc. Palo Alto, California USA); chemical shifts are expressed in  $\delta$  (ppm) and coupling constants (*J*) in hertz. All exchangeable protons were confirmed by addition of D<sub>2</sub>O. *R*<sub>f</sub> values were determined on TLC plates (SiO<sub>2</sub>) using a mixture of DCM/MeOH (92:8, v/v) as eluent.

#### 4.3.1. General procedures for the synthesis of (hetero)aroyl(piperazin-1-yl)methanone derivatives **9a-m**

The intermediates **9a-m** were prepared in two-step one-pot reaction. The first step was conducted following pathway A (for **9a-c** and **9 h-k**) or pathway B (**9d**, **9f-g** and **9 l-m**).

Pathway A: to a solution of 1-Boc-piperazine (**8**) (200 mg, 1.07 mmol) in DCM/DMF (2 mL, 2:1, v/v) placed in a cylindrical quartz tube ( $\varnothing$  2 cm), DIPEA (208  $\mu$ L, 1.6 mmol) and the appropriate aroyl chloride derivatives (1.07 mmol) were added. The mixture was irradiated at room temperature (250 W) for 10 min.

Pathway B: HBTU was added to a solution of the appropriate carboxylic acids (1.07 mmol) in DCM/DMF (2 mL, 2:1, v/v) and placed in a cylindrical quartz tube ( $\varnothing$  2 cm). The mixture was subjected to microwave irradiation at 250 W for 1 min; then, 1-Boc-piperazine (**8**) (200 mg, 1.07 mmol) and DIPEA (208  $\mu$ L, 1.6 mmol) were added and the reaction mixture was irradiated in a microwave oven at 250 W for 25 min.

In the second step, TFA (8.56 mmol) was added at 0 °C and irradiated in a microwave oven 250 W for 5 min. Upon complete *N*-Boc-deprotection, the reaction mixture was cooled into ice and diluted with DCM (2 mL) and 2 M K<sub>2</sub>CO<sub>3</sub> solution (2 mL). The mixture was extracted with DCM (3 × 5 mL), the combined organic layers were dried over Na<sub>2</sub>SO<sub>4</sub>, filtered, and concentrated under vacuo. The residue was treated with Et<sub>2</sub>O giving the desired known intermediates **9a-m**. The chemical properties, as well as the structural assignments, for the resulting compounds **9a-m** were in good agreement with the literature<sup>39–44</sup>. The registered CAS numbers have been already assigned as reported in [Supplementary Material \(Table S2\)](#).

#### 4.3.2. General procedures for the synthesis of 4-(4-(hetero)aroylpiperazine-1-carbonyl)benzenesulfonamide derivatives (**7a-m**)

The activation of the 4-(aminosulfonyl)benzoic acid (1 M equivalent) was conducted by addition of HBTU (1 M equivalent) in dimethylformamide (DMF) (2 mL); the mixture reaction was stirred for 1 h at room temperature. Then, a mixture of TEA (2 M equivalents) and appropriate 4-aroylpiperazine derivatives **9a-m** (1 M equivalent) was added dropwise. The reaction mixture was left overnight at room temperature and then quenched with H<sub>2</sub>O (10 mL) and extracted with EtOAc (3 × 10 mL). The organic phase was washed with saturated NaCl solution, dried with Na<sub>2</sub>SO<sub>4</sub> and concentrated until dryness under reduced pressure. The residue was purified by crystallization from Et<sub>2</sub>O and EtOH to give the desired final compounds **7a-m** as white powder.

#### 4.3.3. 4-(4-(2-Naphthoyl)piperazine-1-carbonyl)benzenesulfonamide (**7a**)

Yield: 56% (286 mg); m.p.: 273–275 °C; R<sub>f</sub>: 0.39. <sup>1</sup>H NMR (500 MHz, DMSO-*d*<sub>6</sub>): (δ) 3.41–3.72 (m, 8H, CH<sub>2</sub>), 7.50 (s, 2H, NH<sub>2</sub>), 7.53–7.65 (m, 5H, ArH), 7.90–8.02 (m, 6H, ArH). <sup>13</sup>C NMR (126 MHz, DMSO-*d*<sub>6</sub>): (δ) 41.9, 47.1, 126.1, 126.9, 127.0, 127.4, 127.5, 127.8, 127.9, 128.4, 128.6, 132.4, 133.1, 133.4, 139.0, 145.2, 168.3, 169.5. Anal. for (C<sub>22</sub>H<sub>21</sub>N<sub>3</sub>O<sub>4</sub>S): C 62.4%, H 5.0%, N 9.9%; Found: C 62.5%, H 4.7%, N 9.6%.

#### 4.3.4. 4-(4-(Thiophene-2-carbonyl)piperazine-1-carbonyl)benzenesulfonamide (**7b**)

Yield: 40% (144 mg); m.p.: 224–226 °C; R<sub>f</sub>: 0.49. <sup>1</sup>H NMR (500 MHz, DMSO-*d*<sub>6</sub>): (δ) 3.41–3.76 (m, 8H, CH<sub>2</sub>), 7.14 (t, J<sub>1</sub> = 3.2 Hz, J<sub>2</sub> = 4.8 Hz, 1H, ArH), 7.45 (d, J = 3.2 Hz, 1H, ArH), 7.48 (bs, 2H, NH<sub>2</sub>), 7.64 (d, J = 8.2 Hz, 2H, ArH), 7.78 (d, J = 4.8 Hz, 1H, ArH), 7.89 (d, J = 8.2 Hz, 2H, ArH). <sup>13</sup>C NMR (126 MHz, DMSO-*d*<sub>6</sub>): (δ) 41.4, 46.4, 125.9, 126.9, 127.4, 127.7, 129.4, 129.7, 132.2, 136.3, 138.6, 144.8, 161.1, 167.9. Anal. for (C<sub>16</sub>H<sub>17</sub>N<sub>3</sub>O<sub>4</sub>S<sub>2</sub>): C 50.6%, H 4.5%, N 11.1%; Found: C 50.5%, H 4.7%, N 10.9%.

#### 4.3.5. 4-(4-(3-Methylthiophene-2-carbonyl)piperazine-1-carbonyl)benzenesulfonamide (**7c**)

Yield: 35% (109 mg); m.p.: 248–250 °C; R<sub>f</sub>: 0.34. <sup>1</sup>H NMR (500 MHz, DMSO-*d*<sub>6</sub>): (δ) 2.20 (m, 3H, CH<sub>3</sub>), 3.54–3.68 (m, 8H, CH<sub>2</sub>), 6.94 (m, 1H, ArH), 7.47 (bs, 2H, NH<sub>2</sub>), 7.62 (m, 1H, ArH), 7.63 (d, J = 8.2 Hz, 2H, ArH), 7.89 (d, J = 8.2 Hz, 2H, ArH). <sup>13</sup>C NMR (126 MHz, DMSO-*d*<sub>6</sub>): 14.3, 41.2, 47.3, 125.7, 126.8, 127.5, 129.8, 129.9, 136.9, 138.6, 144.7, 163.5, 167.9. Anal. for (C<sub>17</sub>H<sub>19</sub>N<sub>3</sub>O<sub>4</sub>S<sub>2</sub>): C 51.9%, H 4.9%, N 10.7%; Found: C 51.7%, H 5.0%, N 10.8%.

#### 4.3.6. 4-(4-(3-Bromothiophene-2-carbonyl)piperazine-1-carbonyl)benzenesulfonamide (**7d**)

Yield: 48% (163 mg); m.p.: 218–220 °C; R<sub>f</sub>: 0.40. <sup>1</sup>H NMR (500 MHz, DMSO-*d*<sub>6</sub>): (δ) 3.39–3.72 (m, 8H, CH<sub>2</sub>), 7.15 (d, J = 5.1 Hz, 1H, ArH), 7.48 (bs, 2H, NH<sub>2</sub>), 7.63–7.65 (m, 2H, ArH), 7.79 (d, J = 5.1 Hz, 1H, ArH), 7.90 (m, 2H, ArH). <sup>13</sup>C NMR (126 MHz, DMSO-*d*<sub>6</sub>): 41.6, 46.9, 109.2, 126.0, 127.8, 127.9, 129.3, 130.0, 130.2, 131.9, 138.9, 145.1, 161.6, 168.2. Anal. for (C<sub>16</sub>H<sub>16</sub>BrN<sub>3</sub>O<sub>4</sub>S<sub>2</sub>): C 41.9%, H 3.5%, N 9.2%; Found: C 41.8%, H 3.7%, N 9.3%.

#### 4.3.7. 4-(4-(5-Chlorothiophen-2-yl)carbonyl)piperazine-1-yl)carbonyl)benzenesulfonamide (**7e**)

Yield: 44% (149 mg); m.p.: 217–219 °C; R<sub>f</sub>: 0.37. <sup>1</sup>H NMR (500 MHz, DMSO-*d*<sub>6</sub>): (δ) 3.68–3.77 (m, 8H, CH<sub>2</sub>), 7.17 (d, J = 3.9 Hz, 1H, ArH), 7.35 (d, J = 3.9 Hz, 1H, ArH), 7.49 (bs, 2H, NH<sub>2</sub>), 7.64 (d, J = 8.2 Hz, 2H, ArH), 7.90 (d, J = 8.2 Hz, 2H, ArH). <sup>13</sup>C NMR (126 MHz, DMSO-*d*<sub>6</sub>): 41.4, 46.4, 125.7, 125.9, 127.0, 127.3, 127.7, 129.5, 132.2, 136.3, 138.6, 144.8, 161.1, 167.9. Anal. for (C<sub>16</sub>H<sub>16</sub>ClN<sub>3</sub>O<sub>4</sub>S<sub>2</sub>): C 46.4%, H 3.9%, N 10.15%; Found: C 46.2%, H 3.7%, N 10.3%.

#### 4.3.8. 4-(4-(5-Nitrothiophen-2-yl)carbonyl)piperazine-1-yl)carbonyl)benzenesulfonamide (**7f**)

Yield: 32% (81 mg); m.p.: 252–254 °C; R<sub>f</sub>: 0.37. <sup>1</sup>H NMR (500 MHz, DMSO-*d*<sub>6</sub>): (δ) 3.43–3.75 (m, 8H, CH<sub>2</sub>), 7.49 (m, 3H, NH<sub>2</sub>, ArH), 7.64 (d, J = 8.2 Hz, 2H, ArH), 7.90 (d, J = 8.2 Hz, 2H, ArH), 8.10 (s, 1H, ArH). <sup>13</sup>C NMR (126 MHz, DMSO-*d*<sub>6</sub>): 41.7, 46.3, 125.9, 127.69, 127.74, 128.68, 128.79, 129.2, 138.8, 143.7, 145.0, 152.3, 160.6, 168.1. Anal. for (C<sub>16</sub>H<sub>16</sub>N<sub>4</sub>O<sub>6</sub>S<sub>2</sub>): C 45.3%, H 3.8%, N 13.2%; Found: C 45.5%, H 3.7%, N 13.5%.

#### 4.3.9. 4-(4-(1-Benzothiophen-2-yl)carbonyl)piperazine-1-yl)carbonyl)benzenesulfonamide (**7g**)

Yield: 43% (232 mg); m.p.: 244–246 °C; R<sub>f</sub>: 0.18. <sup>1</sup>H NMR (500 MHz, DMSO-*d*<sub>6</sub>): (δ) 3.66–3.82 (m, 8H, CH<sub>2</sub>), 7.45–7.46 (m, 3H, ArH), 7.49 (bs, 2H, NH<sub>2</sub>), 7.64 (d, J = 8.2 Hz, 2H, ArH), 7.77 (s, 1H, ArH), 7.90 (d, J = 8.2 Hz, 2H, ArH), 8.01–8.02 (m, 1H, ArH). <sup>13</sup>C NMR (126 MHz, DMSO-*d*<sub>6</sub>): (δ) 41.9, 47.4, 122.8, 125.20, 125.26, 126.06, 126.08, 126.3, 127.9, 128.8, 136.8, 139.0, 139.6, 145.2, 163.0, 168.3. Anal. for (C<sub>20</sub>H<sub>19</sub>N<sub>3</sub>O<sub>4</sub>S<sub>2</sub>): C 55.9%, H 4.5%, N 9.8%; Found: C 55.6%, H 4.3%, N 9.9%.

#### 4.3.10. 4-(4-(Furan-2-carbonyl)piperazine-1-carbonyl)benzenesulfonamide (**7h**)

Yield: 60% (208 mg); m.p.: 211–213 °C; R<sub>f</sub>: 0.68. <sup>1</sup>H NMR (500 MHz, DMSO-*d*<sub>6</sub>): (δ) 3.37–3.79 (m, 8H, CH<sub>2</sub>), 6.64 (m, 1H, ArH), 7.04 (m, 1H, ArH), 7.48 (bs, 2H, NH<sub>2</sub>), 7.64 (d, J = 8.2, 2H, ArH), 7.89 (m, 1H, ArH), 7.90 (d, J = 8.2, 2H, ArH). <sup>13</sup>C NMR (126 MHz, DMSO-*d*<sub>6</sub>): (δ) 42.0, 47.2, 111.6, 116.2, 126.1, 127.9, 139.0, 145.1, 145.2, 146.9, 158.8, 168.3. Anal. for (C<sub>16</sub>H<sub>17</sub>N<sub>3</sub>O<sub>5</sub>S): C 54.1%, H 5.1%, N 11.1%; Found: C 54.3%, H 4.8%, N 10.9%.

#### 4.3.11. 4-(4-(3-Methylfuran-2-yl)carbonyl)piperazine-1-yl)carbonyl)benzenesulfonamide (**7i**)

Yield: 43% (167 mg); m.p.: 189–191 °C; R<sub>f</sub>: 0.43. <sup>1</sup>H NMR (500 MHz, DMSO-*d*<sub>6</sub>): (δ) 2.16 (s, 3H, CH<sub>3</sub>), 3.37–3.69 (m, 8H, CH<sub>2</sub>), 6.50 (m, 1H, ArH), 7.47 (bs, 2H, NH<sub>2</sub>), 7.61–7.68 (m, 3H, ArH), 7.89 (m, 2H, ArH). <sup>13</sup>C NMR (126 MHz, DMSO-*d*<sub>6</sub>): 11.3, 41.9, 47.5, 114.6, 125.9, 126.5, 127.8, 138.9, 142.3, 143.4, 145.0, 159.8, 168.1. Anal. for (C<sub>17</sub>H<sub>19</sub>N<sub>3</sub>O<sub>5</sub>S): C 54.1%, H 5.1%, N 11.1%; Found: C 53.8%, H 5.2%, N 10.9%.

#### 4.3.12. 4-(4-(5-Nitrofuran-2-yl)carbonyl)piperazine-1-yl)carbonyl)benzenesulfonamide (**7j**)

Yield: 38% (102 mg); m.p.: 253–255 °C; R<sub>f</sub>: 0.40. <sup>1</sup>H NMR (500 MHz, DMSO-*d*<sub>6</sub>): (δ) 3.74–3.89 (m, 8H, CH<sub>2</sub>), 7.29 (m, 1H, ArH), 7.48 (bs, 2H, NH<sub>2</sub>), 7.64 (d, J = 8.2, 2H, ArH), 7.76 (m, 1H, ArH), 7.90 (d, J = 8.2, 2H, ArH). <sup>13</sup>C NMR (126 MHz, DMSO-*d*<sub>6</sub>): 42.3, 46.4, 112.7, 112.8, 116.9, 117.2, 125.8, 127.3, 127.6, 138.5, 144.8, 147.2, 151.1, 156.8, 167.9. Anal. for (C<sub>16</sub>H<sub>16</sub>N<sub>4</sub>O<sub>7</sub>S): C 54.1%, H 5.1%, N 11.1%; Found: C 53.7%, H 4.8%, N 11.3%.

#### 4.3.13. 4-(4-(1-Benzofuran-2-yl)carbonyl)piperazine-1-yl)carbonyl)benzenesulfonamide (**7k**)

Yield: 55% (318 mg); m.p.: 209–211 °C; R<sub>f</sub>: 0.24. <sup>1</sup>H NMR (500 MHz, DMSO-*d*<sub>6</sub>): (δ) 3.43–3.84 (m, 8H, CH<sub>2</sub>), 7.33–7.36 (m, 1H, ArH), 7.44–7.49 (m, 4H, NH<sub>2</sub>, ArH), 7.65–7.66 (m, 3H, ArH), 7.75–7.76 (m,

1H, ArH), 7.90–7.92 (m, 2H, ArH). <sup>13</sup>C NMR (126 MHz, DMSO-*d*<sub>6</sub>): 41.8, 47.2, 111.4, 112.0, 122.6, 123.9, 126.0, 126.8, 127.8, 138.9, 145.1, 148.1, 154.1, 159.2, 168.2. Anal. for (C<sub>20</sub>H<sub>19</sub>N<sub>3</sub>O<sub>5</sub>S): C 58.1%, H 4.6%, N 10.2%; Found: C 58.3%, H 4.8%, N 10.1%.

#### 4.3.14. 4-(4-(1H-Pyrrole-2-carbonyl)piperazine-1-carbonyl)benzenesulfonamide (7 I)

Yield: 62% (279 mg); m.p.: 247–249 °C; R<sub>f</sub>: 0.42. <sup>1</sup>H NMR (500 MHz, DMSO-*d*<sub>6</sub>): (δ) 3.71–3.81 (m, 8H, CH<sub>2</sub>), 6.12 (m, 1H, ArH), 6.53 (m, 1H, ArH), 6.90 (m, 1H, ArH), 7.49 (bs, 2H, NH<sub>2</sub>), 7.64 (d, J = 8.2, 2H, ArH), 7.90 (d, J = 8.2, 2H, ArH), 11.47 (bs, 1H, NH). <sup>13</sup>C NMR (126 MHz, DMSO-*d*<sub>6</sub>): (δ) 41.9, 47.2, 108.5, 108.7, 112.1, 112.4, 121.5, 121.7, 124.0, 125.6, 125.8, 127.7, 138.9, 144.7, 161.6, 168.1. Anal. for (C<sub>16</sub>H<sub>18</sub>N<sub>4</sub>O<sub>4</sub>S): C 53.0%, H 5.0%, N 15.5%; Found: C 53.1%, H 5.2%, N 15.3%.

#### 4.3.15. 4-(4-(1H-Indole-2-carbonyl)piperazine-1-carbonyl)benzenesulfonamide (7 M)

Yield: 73% (209 mg); m.p.: 239–241 °C; R<sub>f</sub>: 0.42. <sup>1</sup>H NMR (500 MHz, DMSO-*d*<sub>6</sub>): (δ) 3.22–4.00 (m, 8H, CH<sub>2</sub>), 6.84 (bs, 1H, NH), 7.03–7.06 (m, 1H, ArH), 7.18–7.21 (m, 1H, ArH), 7.44–7.61 (m, 4H, ArH, NH<sub>2</sub>), 7.65–7.66 (m, 2H, ArH), 7.91–7.94 (m, 2H, ArH), 11.66 (bs, 1H, NH). <sup>13</sup>C NMR (126 MHz, DMSO-*d*<sub>6</sub>): 41.6, 46.7, 104.3, 112.0, 119.7, 121.3, 125.8, 126.7, 127.5, 135.9, 138.7, 141.2, 144.9, 162.1, 167.9. Anal. for C<sub>20</sub>H<sub>20</sub>N<sub>4</sub>O<sub>5</sub>S: C 58.2%; H 4.9%; N 13.6%. Found: C 58.1%; H 5.0%; N 13.4%.

#### 4.4. CA inhibition assay

An Applied Photophysics stopped-flow instrument has been used for assaying the CA catalysed CO<sub>2</sub> hydration activity. Phenol red (at a concentration of 0.2 mM) has been used as indicator, working at the absorbance maximum of 557 nm, with 10 – 20 mM Hepes (pH 7.5) as buffer, and 20 mM Na<sub>2</sub>SO<sub>4</sub> or 20 mM NaClO<sub>4</sub> (for maintaining constant the ionic strength), following the initial rates of the CA-catalyzed CO<sub>2</sub> hydration reaction for a period of 10–100 s. The CO<sub>2</sub> concentrations ranged from 1.7 to 17 mM for the determination of the kinetic parameters and inhibition constants. For each inhibitor at least six traces of the initial 5–10% of the reaction have been used for determining the initial velocity. The uncatalyzed rates were determined in the same manner and subtracted from the total observed rates. Stock solutions of inhibitor (10 mM) were prepared in distilled-deionized water and dilutions up to 0.01 nM were done thereafter with distilled-deionized water. Inhibitor and enzyme solutions were preincubated together for 15 min at room temperature prior to assay, in order to allow for the formation of the E-I complex. The inhibition constants were obtained by non-linear least-squares methods using PRISM 3, as reported earlier, and represent the mean from at least three different determinations. CA isoforms were recombinant ones obtained as reported earlier by this group and their concentration in the assay system was of 5–10 nM.<sup>5,6,45</sup>

#### Declaration of Competing Interest

The authors declare that they have no known competing financial interests or personal relationships that could have appeared to influence the work reported in this paper.

#### Acknowledgment

We acknowledge the financial support for this research by MIUR (grant number PRIN2017\_201744BN5T). We thank Mr. Maurizio Amendola for his skilful technical assistance with X-ray measurements.

#### Appendix A. Supplementary material

Supplementary data to this article can be found online at <https://doi.org/10.1016/j.bmc.2021.116279>.

[org/10.1016/j.bmc.2021.116279](https://doi.org/10.1016/j.bmc.2021.116279).

#### References

- Alterio V, Di Fiore A, D'Ambrosio K, Supuran CT, De Simone G. Multiple binding modes of inhibitors to carbonic anhydrases: how to design specific drugs targeting 15 different isoforms? *Chem Rev*. 2012;112(8):4421–4468.
- Supuran CT. Advances in structure-based drug discovery of carbonic anhydrase inhibitors. *Expert Opin Drug Discov*. 2017;12(1):61–88.
- Supuran CT. Carbonic anhydrases: novel therapeutic applications for inhibitors and activators. *Nat Rev Drug Discov*. 2008;7(2):168–181.
- Monti SM, Supuran CT, De Simone G. Anticancer carbonic anhydrase inhibitors: a patent review (2008–2013). *Expert Opin Ther Pat*. 2013;23(6):737–749.
- Nishimori I, Vullo D, Innocenti A, Scozzafava A, Mastrolorenzo A, Supuran CT. Carbonic anhydrase inhibitors: inhibition of the transmembrane isozyme XIV with sulfonamides. *Bioorg Med Chem Lett*. 2005;15(17):3828–3833.
- Nishimori I, Vullo D, Innocenti A, Scozzafava A, Mastrolorenzo A, Supuran CT. Carbonic anhydrase inhibitors. The mitochondrial isozyme VB as a new target for sulfonamide and sulfamate inhibitors. *J Med Chem*. 2005;48(24):7860–7866.
- Ruusuvuori E, Kaila K. Carbonic anhydrases and brain pH in the control of neuronal excitability. *Sub-cellular biochemistry*. 2014;75:271–290.
- Supuran CT. Carbonic anhydrase inhibitors as emerging drugs for the treatment of obesity. *Expert Opin Emerg Drugs*. 2012;17(1):11–15.
- Bonardi A, Falsini M, Catarzi D, et al. Structural investigations on coumarins leading to chromeno[4,3-*c*]pyrazol-4-ones and pyrano[4,3-*c*]pyrazol-4-ones: New scaffolds for the design of the tumor-associated carbonic anhydrase isoforms IX and XII. *Eur J Med Chem*. 2018;146:47–59.
- Supuran CT, Di Fiore A, De Simone G. Carbonic anhydrase inhibitors as emerging drugs for the treatment of obesity. *Expert Opin Emerg Drugs*. 2008;13(2):383–392.
- Waheed A, Sly WS. Carbonic anhydrase XII functions in health and disease. *Gene*. 2017;623:33–40.
- Lomelino CL, Andring JT, McKenna R. Crystallography and Its Impact on Carbonic Anhydrase Research. *Int J Med Chem*. 2018;2018:9419521.
- Bruno E, Buemi MR, De Luca L, et al. In Vivo Evaluation of Selective Carbonic Anhydrase Inhibitors as Potential Anticonvulsant Agents. *ChemMedChem*. 2016;11(16):1812–1818.
- De Luca L, Ferro S, Damiano FM, et al. Structure-based screening for the discovery of new carbonic anhydrase VII inhibitors. *Eur J Med Chem*. 2014;71:105–111.
- Gitto R, Agnello S, Ferro S, Vullo D, Supuran CT, Chimirri A. Identification of potent and selective human carbonic anhydrase VII (hCA VII) inhibitors. *ChemMedChem*. 2010;5(6):823–826.
- Abo-Ashour MF, Eldehna WM, Nocentini A, et al. Novel synthesized SLC-0111 thiazole and thiazole analogues: Determination of their carbonic anhydrase inhibitory activity and molecular modeling studies. *Bioorg Chem*. 2019;87:794–802.
- Andreucci E, Ruzzolini J, Peppicelli S, et al. The carbonic anhydrase IX inhibitor SLC-0111 sensitises cancer cells to conventional chemotherapy. *J Enzyme Inhib Med Chem*. 2019;34(1):117–123.
- Boyd NH, Walker K, Fried J, et al. Addition of carbonic anhydrase 9 inhibitor SLC-0111 to temozolomide treatment delays glioblastoma growth in vivo. *JCI Insight*. 2017;2(24).
- Bozdag M, Carta F, Ceruso M, et al. Discovery of 4-Hydroxy-3-(3-(phenylureido)benzenesulfonamides as SLC-0111 Analogues for the Treatment of Hypoxic Tumors Overexpressing Carbonic Anhydrase IX. *J Med Chem*. 2018;61(14):6328–6338.
- Carta F, Vullo D, Osman SM, AlOthman Z, Supuran CT. Synthesis and carbonic anhydrase inhibition of a series of SLC-0111 analogs. *Bioorg Med Chem*. 2017;25(9):2569–2576.
- Eldehna WM, Abo-Ashour MF, Berrino E, et al. SLC-0111 enamino analogs, 3/(4-(3-aryl-3-oxopropenyl)aminobenzenesulfonamides, as novel selective subnanomolar inhibitors of the tumor-associated carbonic anhydrase isoform IX. *Bioorg Chem*. 2019;83:549–558.
- Eldehna WM, Abo-Ashour MF, Nocentini A, et al. Enhancement of the tail hydrophobic interactions within the carbonic anhydrase IX active site via structural extension: Design and synthesis of novel N-substituted isatin-SLC-0111 hybrids as carbonic anhydrase inhibitors and antitumor agents. *Eur J Med Chem*. 2019;162:147–160.
- Lomelino CL, Mahon BP, McKenna R, Carta F, Supuran CT. Kinetic and X-ray crystallographic investigations on carbonic anhydrase isoforms I, II, IX and XII of a thioureido analog of SLC-0111. *Bioorg Med Chem*. 2016;24(5):976–981.
- Supuran CT. Experimental Carbonic Anhydrase Inhibitors for the Treatment of Hypoxic Tumors. *J Exp Pharmacol*. 2020;12:603–617.
- Angeli A, Carta F, Nocentini A, et al. Carbonic Anhydrase Inhibitors Targeting Metabolism and Tumor Microenvironment. *Metabolites*. 2020;10(10).
- Bruno E, Buemi MR, Di Fiore A, et al. Probing Molecular Interactions between Human Carbonic Anhydrases (hCAs) and a Novel Class of Benzenesulfonamides. *J Med Chem*. 2017;60(10):4316–4326.
- Buemi MR, De Luca L, Ferro S, et al. Carbonic anhydrase inhibitors: Design, synthesis and structural characterization of new heteroaryl-N-carbonylbenzenesulfonamides targeting druggable human carbonic anhydrase isoforms. *Eur J Med Chem*. 2015;102:223–232.
- Mancuso F, Di Fiore A, De Luca L, et al. Looking toward the Rim of the Active Site Cavity of Druggable Human Carbonic Anhydrase Isoforms. *ACS Med Chem Lett*. 2020;11(5):1000–1005.
- Buemi MR, Di Fiore A, De Luca L, et al. Exploring structural properties of potent human carbonic anhydrase inhibitors bearing a 4-(cycloalkylamino-1-carbonyl)benzenesulfonamide moiety. *Eur J Med Chem*. 2019;163:443–452.

- 30 Di Fiore A, Truppo E, Supuran CT, et al. Crystal structure of the C183S/C217S mutant of human CA VII in complex with acetazolamide. *Bioorg Med Chem Lett.* 2010; 20(17):5023–5026.
- 31 Otwinowski Z, Minor W. Processing of X-ray diffraction data collected in oscillation mode. *Methods Enzymol.* 1997;276:307–326.
- 32 Buonanno M, Di Fiore A, Langella E, et al. The Crystal Structure of a hCA VII Variant Provides Insights into the Molecular Determinants Responsible for Its Catalytic Behavior. *Int J Mol Sci.* 2018;19(6).
- 33 Brunger AT. Version 1.2 of the Crystallography and NMR system. *Nat Protoc.* 2007;2(11):2728–2733.
- 34 Brunger AT, Adams PD, Clore GM, et al. Crystallography & NMR system: A new software suite for macromolecular structure determination. *Acta Crystallogr D Biol Crystallogr.* 1998;54(Pt 5):905–921.
- 35 Jones G, Willett P, Glen RC, Leach AR, Taylor R. Development and validation of a genetic algorithm for flexible docking. *J Mol Biol.* 1997;267(3):727–748.
- 36 Hoof RW, Vriend G, Sander C, Abola EE. Errors in protein structures. *Nature.* 1996; 381(6580):272.
- 37 Laskowski RA, MacArthur MW, Moss DS, Thornton JM. Procheck - a Program to Check the Stereochemical Quality of Protein Structures. *J Appl Crystallogr.* 1993;26: 283–291.
- 38 Pedretti A, Villa L, Vistoli G. VEGA: a versatile program to convert, handle and visualize molecular structure on Windows-based PCs. *J Mol Graph Model.* 2002;21(1): 47–49.
- 39 Zulli AL, Aimone LD, Mathiasen JR, et al. Substituted phenoxypropyl-(R)-2-methylpyrrolidine aminomethyl ketones as histamine-3 receptor inverse agonists. *Bioorg Med Chem Lett.* 2012;22(8):2807–2810.
- 40 Qin Q, Wu T, Yin W, et al. Discovery of 2,4-diaminopyrimidine derivatives targeting p21-activated kinase 4: Biological evaluation and docking studies. *Arch Pharm (Weinheim).* 2020;353(10), e2000097.
- 41 Moussa IA, Banister SD, Beinat C, Giboureau N, Reynolds AJ, Kassiou M. Design, synthesis, and structure-affinity relationships of regioisomeric N-benzyl alkyl ether piperazine derivatives as sigma-1 receptor ligands. *J Med Chem.* 2010;53(16): 6228–6239.
- 42 Moritz AE, Free RB, Weiner WS, et al. Discovery, Optimization, and Characterization of ML417: A Novel and Highly Selective D3 Dopamine Receptor Agonist. *J Med Chem.* 2020;63(10):5526–5567.
- 43 Drizin I, Gregg RJ, Scanio MJ, et al. Discovery of potent furan piperazine sodium channel blockers for treatment of neuropathic pain. *Bioorg Med Chem.* 2008;16(12): 6379–6386.
- 44 Akbar A, McNeil NMR, Albert MR, et al. Structure-Activity Relationships of Potent, Targeted Covalent Inhibitors That Abolish Both the Transamidation and GTP Binding Activities of Human Tissue Transglutaminase. *J Med Chem.* 2017;60(18):7910–7927.
- 45 Innocenti A, Vullo D, Pastorek J, et al. Carbonic anhydrase inhibitors. Inhibition of transmembrane isozymes XII (cancer-associated) and XIV with anions. *Bioorg Med Chem Lett.* 2007;17(6):1532–1537.